

Cite this: *Chem. Sci.*, 2023, **14**, 4627 All publication charges for this article have been paid for by the Royal Society of ChemistryReceived 1st March 2023
Accepted 5th April 2023DOI: 10.1039/d3sc01126g
rsc.li/chemical-science

Introduction

The cyanide ion ($\text{C}\equiv\text{N}^-$) is found in coordination compounds across many areas of chemistry, ranging from biological enzyme cofactors to bespoke magnetic materials and catalysts.^{1–4} In the end-on κC coordination mode, the cyanide ion is an archetypal strong field ligand, a good σ donor and moderate π acceptor. These properties are critical to the utility of the cyanido ligand; its uncommon ability to withdraw π electron density despite its negative charge makes it a particularly useful tool in coordination chemistry.^{5–7}

The cyaphide ion, $\text{C}\equiv\text{P}^-$, is a phosphorus-containing analogue of the cyanide ion. Unlike the cyanide ion, it is rare, with relatively few known examples of cyaphido metal complexes having been reported to date.^{8–12} As a consequence, its ligand properties are still poorly understood. However, the potential for even higher π accepting character compared to cyanide has made the cyaphide ion an attractive candidate for use as a bridging ligand in magnetic materials, where its low-lying $\text{C}\equiv\text{P}$ π^* orbitals should facilitate more effective super-exchange between open-shell metal centers.⁶ Conceptually, the cyaphide ion is most closely related to two isolobal congeners, the cyanide ($\text{C}\equiv\text{N}^-$) and acetylido ($\text{C}\equiv\text{CH}^-$) ions. While both the cyanido and acetylido ligands are known to be good σ

donors, the acetylido ligand has much reduced π withdrawing character, acting as a borderline π acceptor or donor.^{13,14}

There is scant experimental evidence available with which to probe the electronic properties of the cyaphido ligand. The only systematic study of κC -cyaphido complexes conducted to date exclusively probed the effect of *trans*-ligated acetylides on ruthenium(II) cyaphido complexes,¹⁵ leaving the donor/acceptor properties of the cyaphide ligand itself still somewhat of a mystery.

Recently, we reported a magnesium(II) cyaphide complex $\text{Mg}^{(\text{DippNacNac})(\text{dioxane})(\text{CP})}$ (**Mg_{CP}**; $\text{DippNacNac} = \text{CH}(\text{C}(\text{CH}_3)\text{N}(\text{Dipp})_2$ and $\text{Dipp} = 2,6\text{-diisopropylphenyl}$) which, by analogy to Grignard reagents, can be used to transfer the cyaphide ion to the coordination sphere of other metal centers using simple salt metathesis reactions.¹⁶ This has enabled synthetic access to many metal cyaphido coordination complexes which can be studied to better understand the properties of this anion. To this end, we recently used the gold(I) cyaphide complex $\text{Au}(\text{I-Dipp})(\text{CP})$ (**Au_{CP}**; $\text{IDipp} = 1,3\text{-bis}(\text{diisopropylphenyl})\text{-imidazol-2-ylidene}$) to prepare heterometallic complexes featuring the cyaphide ion as a bridging ligand, revealing the electrophilic, π withdrawing nature of the cyaphide ion in side-on η^2 -coordination to metal centers (Fig. 1).¹⁷

As traditional methods for probing ligand donor strength are currently inaccessible for the cyaphido ligand – due to a lack of $[\text{M}(\text{CP})_6]^{x-}$ or $[\text{M}(\text{CP})_4]^{x-}$ type complexes – in this study we focus on the use of both NMR spectroscopic and crystallographically determined bond metric data to do so. This allows us to deconvolute the donor/acceptor properties of the terminal κC -cyaphido ligand through comparative studies of three cyaphido metal complexes, the gold(I) complex $(\text{IDipp})\text{Au}(\text{CP})$ (**Au_{CP}**), the cobalt(I) complex $\text{Co}^{(\text{DippPDI})(\text{CP})}$ (**Co_{CP}**; $\text{DippPDI} = 1,1'\text{-}(\text{pyridine-2,6-diyl})\text{bis}(\text{N}-\text{2,6-diisopropylphenyl})\text{ethan-1-imine}$), and

^aDepartment of Chemistry, University of Oxford, Chemistry Research Laboratory, 12 Mansfield Rd., Oxford, OX1 3TA, UK

^bDepartment of Chemistry, Indiana University, 800 East Kirkwood Ave., Bloomington, Indiana, 47405, USA. E-mail: jgoicoec@iu.edu

† Electronic supplementary information (ESI) available. CCDC 2242900–2242911. For ESI and crystallographic data in CIF or other electronic format see DOI: <https://doi.org/10.1039/d3sc01126g>



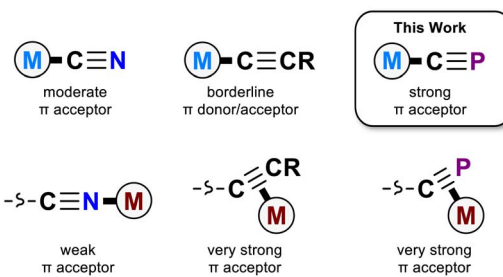


Fig. 1 Coordination chemistry of the cyanido, acetylido, and cyaphido ligands.

the novel rhodium(i) complex $\text{Rh}^{(\text{DippPDI})}(\text{CP})$ (**Rh_{CP}**). **Au_{CP}** is compared to other known gold(i) complexes $\text{Au}(\text{IDipp})\text{X}$ and $[\text{Au}(\text{Dipp})\text{L}]^+$ (**Au_X** and **Au_L**; where X and L are used to describe anionic and neutral ligands, respectively, in accordance with the Covalent Bond Classification Method).¹⁸ Analysis of the gold(i) complexes allows us to determine the σ donor properties of the cyaphide ion. A systematic comparison of **Co_{CP}** and **Rh_{CP}** with both known and novel $\text{M}^{(\text{DippPDI})}\text{X}$ and $[\text{M}^{(\text{DippPDI})}\text{L}]^+$ complexes (**M_X** and **M_L**, M = Co, Rh) allows us to probe the π accepting character of the terminally bonded cyaphido ligand.

Results and discussion

From a theoretical standpoint, the ligand properties of the cyaphide ion are not immediately obvious. Its 2p-3p C≡P π bonds result both in low energy antibonding π^* orbitals (6.69 eV, cf. CN^- : 9.34 eV, CCH^- : 8.98 eV) as well as high energy bonding π orbitals (-3.36 eV, cf. CN^- : -4.47 eV, CCH^- : -3.08 eV), increasing both π withdrawing and π donating ability relative to the cyanide ion. Moreover, the lower electronegativity of phosphorus relative to carbon results in the polarization of the π^* orbital away from the coordinating carbon atom (41.0% C, cf. CN^- : 79.3% C, CCH^- : 48.5% C), in principle worsening $\text{Md}-\pi^*$ orbital overlap (Fig. 2, see ESI† for full computational details).

It has been previously demonstrated that the N-heterocyclic carbene (NHC) carbenoid $^{13}\text{C}\{^1\text{H}\}$ NMR chemical shift ($^{13}\text{C}_{\text{NHC}}$) is sensitive to the σ basicity of *trans*-coordinated co-ligands.¹⁹ A

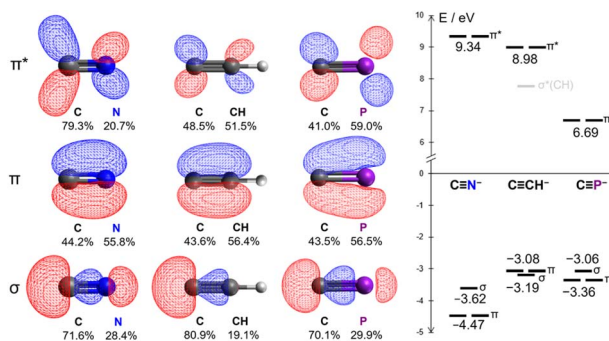


Fig. 2 Kohn–Sham DFT frontier orbitals of the cyanide, acetylido, and cyaphide ions.

similar trend can be observed in the case of gold(i) $\text{Au}(\text{IDipp})\text{X}$ and $[\text{Au}(\text{Dipp})\text{L}]^+$ complexes (**Au_X** and **Au_L**) which exhibit $^{13}\text{C}_{\text{NHC}}$ chemical shifts over a wide frequency range (~50 ppm) depending on the nature of the ligand *trans* to the carbene (Table S9†).^{16,17,20–28} Weak σ donors (such as acetonitrile) give rise to low $^{13}\text{C}_{\text{NHC}}$ chemical shifts (e.g. $\text{Au}_{\text{NCMe}}^+$: $^{13}\text{C}_{\text{NHC}} = 166.0$ ppm), whereas strong donors (e.g. boryls) give rise to high shifts (e.g. $\text{Au}_{\text{BPiN}}^+$: $^{13}\text{C}_{\text{NHC}} = 216.7$ ppm). The solid-state $\text{C}_{\text{NHC}}-\text{Au}$ bond lengths in such complexes are less sensitive to the nature of the *trans*-ligand, although they follow a similar trend, apart from strong π donors (such as chloride and hydroxide ligands) which deviate slightly. This is consistent with previous theoretical studies on gold(i) NHC complexes: while electrostatic and σ donation effects dominate for NHC–Au^I bonds,²⁹ π donating coligands have been shown to enable more significant Au^I–NHC π backbonding.³⁰

EDA-NOCV analysis of the L–Au bond in the aforementioned complexes allows for the theoretical examination of σ donor and π acceptor orbital interactions. Experimental $^{13}\text{C}_{\text{NHC}}$ chemical shifts correlate very well with calculated ETS-NOCV σ donation energies (Fig. 3), and conversely do not correlate well with ETS-NOCV π backdonation energies (Fig. S50†). Thus the $^{13}\text{C}_{\text{NHC}}$ chemical shift in $\text{Au}(\text{IDipp})\text{X}$ and $[\text{Au}(\text{Dipp})\text{L}]^+$ compounds can be taken as a measure of the σ donating ability of the *trans* ligand.

In **Au_{CP}**, the $^{13}\text{C}_{\text{NHC}}$ chemical shift is 193.0 ppm, in a very similar range to other sp-hybridized carbanions such as cyanide and phenylacetylide (Au_{CN}^+ : $^{13}\text{C}_{\text{NHC}} = 186.2$ ppm; $\text{Au}_{\text{CCPh}}^+$: $^{13}\text{C}_{\text{NHC}} = 190.0$ ppm). This is also reflected computationally in the ETS-NOCV σ donor energies: the cyaphide complex has a $\Delta E_{\text{orb}}^{\sigma}$ value of -44.5 kcal mol⁻¹ compared to -40.8 kcal mol⁻¹ for cyanide and -42.5 kcal mol⁻¹ for acetylido. These data show that the cyaphido ligand has a very similar σ basicity to closely related

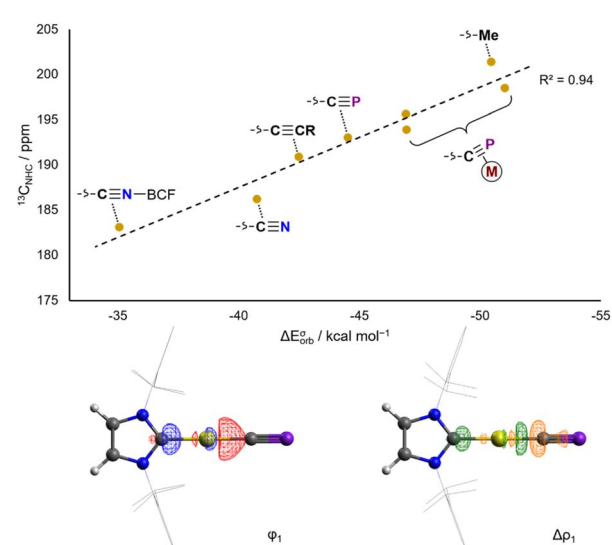


Fig. 3 Correlation of calculated ETS-NOCV σ donation energies with experimental $^{13}\text{C}_{\text{NHC}}$ NMR spectroscopic data for Au_X complexes (top). Isosurfaces for the σ bonding NOCV and difference density in Au_{CP} (bottom).

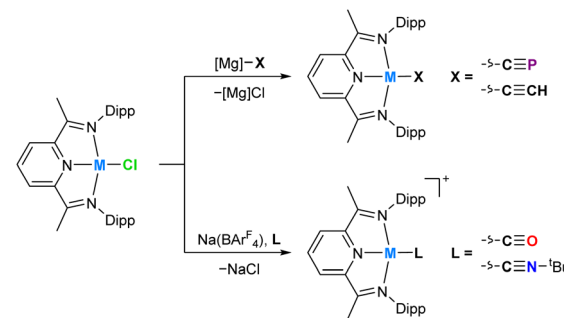


sp-carbanionic ligands, though slightly higher due to its higher energy HOMO and/or the lower electronegativity of phosphorus resulting in higher charge density at carbon.

The same analysis can be performed for the previously reported hetero- bi- and tri-metallic bridging cyaphide complexes $\{\text{Au}(\text{IDipp})\}\{\text{Ni}(\text{Me}^+\text{iPr})_2\}(\mu\text{-CP})$, $\{\text{Au}(\text{IDipp})\}\{\text{Rh}(\text{Cp}^*)(\text{PMe}_3)\}(\mu\text{-CP})$, and $\{\text{Au}(\text{IDipp})\}\{\text{Rh}(\text{Cp}^*)(\text{PMe}_3)\}\{\text{W}(\text{CO})_5\}(\mu\text{-CP})$.¹⁷ The bimetallic complexes give rise to higher $^{13}\text{C}_{\text{NHC}}$ chemical shifts ($^{13}\text{C}_{\text{NHC}} = 198.5$ and 195.6 ppm, for the nickel and rhodium complexes, respectively), showing that the net electron-withdrawing nature of the η^2 cyaphido-metal interaction results in heightened σ donor ability at carbon, which is also reflected in larger calculated $\Delta E_{\text{orb}}^{\sigma}$ energies ($\Delta E_{\text{orb}}^{\sigma} = -51.0$ and -46.9 kcal mol $^{-1}$, respectively). Coordination of a third metal to the cyaphide ion *via* the phosphorus lone pair results in a moderate reduction in σ donor ability, with the trimetallic complex exhibiting a $^{13}\text{C}_{\text{NHC}}$ chemical shift of 193.9 ppm.

Whereas Au_{CP} allows for the study of the σ donor properties of the κC -cyaphido ligand, the group 9 cyaphido complexes $\text{Co}^{(\text{DippPDI})}(\text{CP})$ (Co_{CP}) and $\text{Rh}^{(\text{DippPDI})}(\text{CP})$ (Rh_{CP}) are sensitive to its π donor/acceptor character. The tridentate pyridine diimine (PDI) ligand framework has a low lying π^* orbital that gives rise to strong π accepting character and redox non-innocence. Population of this π^* orbital by π backdonation or reduction results in measurable changes in the solid-state bond metrics of the PDI ligand, summarized in the parameter $\delta(\text{PDI})$,³¹ which allows for convenient assessment of the electronic structure of metal PDI complexes (see Tables S10 and S11†). An NMR study of the purple, square-planar cobalt complexes $\text{Co}^{(\text{DippPDI})}\text{H}$ (Co_{H}), $\text{Co}^{(\text{DippPDI})}\text{Me}$ (Co_{Me}),³² and $\text{Co}^{(\text{DippPDI})}\text{Cl}$ (Co_{Cl}),³³ has previously shown that they consist of cobalt(II) centers ligated by reduced $(\text{DippPDI})^{\cdot-}$ radical anions.³⁴ Notably absent from this study were ligands with appreciable π accepting ability. Indeed it has been noted that the cationic dinitrogen complex $[\text{Co}^{(\text{DippPDI})}(\text{N}_2)]^+[\text{B}(\text{Me})(\text{C}_6\text{F}_5)_3]$ has a markedly different $\delta(\text{PDI})$ value than for the aforementioned complexes (0.132(9); *cf.* 0.090(9)–0.098(7) for Co_{H} , Co_{Me} , and Co_{Cl}) and is a deep blue color instead of purple. This suggests it is better described as having a cobalt(I) center and neutral DippPDI ligand.³¹

In order to provide additional useful data points against which the cobalt(I) cyaphide complex Co_{CP} can be compared, several complexes with ligands of varying π acceptor character (Co_X and Co_L^+) were prepared and characterized.‡ The purple cobalt acetylidyne complex $\text{Co}^{(\text{DippPDI})}(\text{CCH})$ (Co_{CCH}) was prepared by salt metathesis of Co_{Cl} with ethynylmagnesium chloride (Scheme 1). Its solid-state structure was determined by single crystal X-ray diffraction (Fig. 4), showing a square-planar cobalt center with a $\text{N}_{\text{py}}\text{-Co}$ bond length of $1.812(2)$ Å and a $\delta(\text{PDI})$ value of $0.098(7)$ (Table S10†). If the reaction is performed with an excess of sodium acetylidyne instead of the Grignard reagent, a mixture of products forms, from which $\text{Na}(\text{THF})\text{Co}(\text{PIEA})(\text{CCH})$ (PIEA = pyridine-imine-enamine) can be isolated, containing a deprotonated PDI ligand and a sodium cation held in a close ion pair by π interactions with arene and acetylidyne moieties.



Scheme 1 Synthesis of M_X ($\text{M} = \text{Co, Rh}$; $X = \text{CP}^-$, CCH^-) and M_L^+ complexes ($\text{M} = \text{Co, Rh}$; $L = \text{CO, CN}^{\text{tBu}}$).

Cobalt carbonyl $[\text{Co}^{(\text{DippPDI})}(\text{CO})][\text{BArF}_4]$ (Co_{CO}^+ , BArF_4^- = tetrakis(3,5-bis(trifluoromethyl)phenyl)borate) and *tert*-butyl isocyanide $[\text{Co}^{(\text{DippPDI})}(\text{CN}^{\text{tBu}})][\text{BArF}_4]$ ($\text{Co}_{\text{CNBu}}^+$) complexes were synthesized by halide abstraction with $\text{Na}(\text{BArF}_4)$ in 1,2-difluorobenzene (1,2-DFB), in the presence of CO gas or $^{\text{t}}\text{BuNC}$, respectively. Both complexes are blue and have solid-state structures with $\text{N}_{\text{py}}\text{-Co}$ bond lengths of $1.847(2)$ Å (Co_{CO}^+) and $1.819(2)$ Å ($\text{Co}_{\text{CNBu}}^+$), and $\delta(\text{PDI})$ values of $0.144(7)$ (Co_{CO}^+) and $0.121(4)$ ($\text{Co}_{\text{CNBu}}^+$). If two equivalents of $^{\text{t}}\text{BuNC}$ are used the reaction results in a different product, $[\text{Co}^{(\text{DippPDI})}(\text{CN}^{\text{tBu}})_2][\text{BArF}_4]$ ($\text{Co}_{2\text{CNBu}}^+$), with a five-coordinate square-pyramidal cobalt center (see ESI†).

The cobalt cyanide complex $\text{Co}^{(\text{DippPDI})}(\text{CN})$ (Co_{CN}) was also targeted, although attempts to prepare it *via* several methods were unsuccessful, including salt metathesis with KCN or

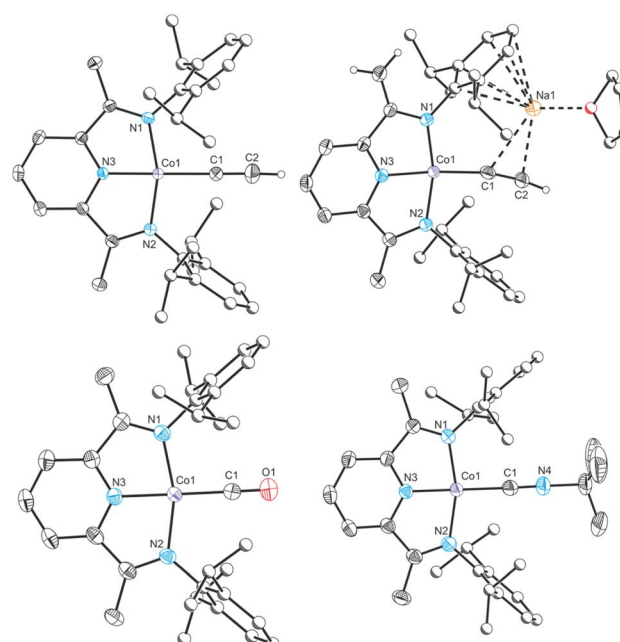


Fig. 4 Clockwise from top left: single crystal X-ray structures of complexes Co_{CCH} , $\text{Na}(\text{THF})\text{Co}(\text{PIEA})(\text{CCH})$, $\text{Co}_{\text{CNBu}}^+$ and Co_{CO}^+ . Thermal ellipsoids set at 50% probability level. Hydrogen atoms (except for acetylidyne and terminal alkene protons) removed for clarity. Atoms of Dipp groups pictured as spheres of arbitrary radius.



Me₃SiCN, and halide abstraction in the presence of [Bu₄N]CN. This is likely due to the potential for redox disproportionation. The reaction of the cobalt(II) complex Co(^{DiPP}PDI)Cl₂ with sodium cyanide was previously shown to lead to disproportionation, forming Co(^{DiPP}PDI)(CN)₃ and other unidentified byproducts.³⁵ An alternative decomposition pathway could involve deprotonation of the PDI ligand by the Brønsted basic cyanide ion (as observed for the reaction of **CoCl** with sodium acetylidyde; *vide supra*).

The cobalt cyaphide complex **Co_{CP}** is blue, with a N_{py}–Co bond length of 1.825(3) Å and a δ (PDI) value of 0.131(9). From these data, it is clear that **Co_X** and **Co_L⁺** (X and L are CP[−], CCH[−], Me[−], N₂, CO, CN[−]Bu, and Cl[−]) can be separated into two groups with different electronic structures. The purple complexes with low δ (PDI) values are best described as Co²⁺(^{DiPP}PDI)[−] systems, whereas the blue complexes with high δ (PDI) values are better described as Co¹⁺(^{DiPP}PDI). In order to quantify this, UV-vis spectra for all complexes were measured. As expected, the absorbance maxima (λ_{max}) relate discontinuously with δ (PDI), with low λ_{max} corresponding to low δ (PDI) and *vice versa* (Fig. 5).

The group of blue Co¹⁺(^{DiPP}PDI) complexes with higher λ_{max} and δ (PDI) values all feature π accepting ligands, with the notable inclusion of the cyaphide ion. This can be rationalized by considering the effect of the ligand on the Co(^{DiPP}PDI) fragment: when it is primarily electron donating, the electron rich Co(^{DiPP}PDI) fragment favors the reduced ^{DiPP}PDI state, whereas when the ligand is π withdrawing, the less electron rich Co(^{DiPP}PDI) fragment favors the neutral ^{DiPP}PDI state.

In order to better quantify the π accepting ability of the cyaphido ligand, the heavier group 9 ^{DiPP}PDI complexes Rh(^{DiPP}PDI)X and [Rh(^{DiPP}PDI)L]⁺ (**Rh_X** and **Rh_L⁺**) were prepared, in which the much lower relative favorability of the rhodium(II) oxidation state should preclude the redox non-innocence of the PDI ligand. Addition of Rh(^{DiPP}PDI)Cl³⁶ (**Rh_{Cl}**) to a toluene solution of the cyaphide transfer reagent **Mg_{CP}** results in the formation of the novel rhodium(I) cyaphide complex Rh(^{DiPP}PDI)(CP) (**Rh_{CP}**) after 3 days. **Rh_{CP}** exhibits a doublet in its ³¹P{¹H} NMR spectrum at 251.4 ppm ($^2J_{\text{P-Rh}} = 6$ Hz) corresponding to the cyaphide phosphorus atom and a doublet of doublets in its ¹³C{¹H} NMR spectrum at 264.15 ppm ($^1J_{\text{C-Rh}} = 54.8$ Hz, $^1J_{\text{C-P}} = 22.9$ Hz) corresponding to the cyaphide carbon atom. The C≡P vibrational stretching

frequency was measured to be 1334 cm^{−1} by Raman spectroscopy (*cf.* 1306 cm^{−1} for **Co_{CP}**). Its solid-state structure was determined by X-ray crystallography (Fig. 6), revealing a square-planar rhodium center, a C–P bond length of 1.542(4) Å (*cf.* 1.506(4) Å for **Co_{CP}**), a N_{py}–Rh bond length of 1.943(2) Å, and a δ (PDI) value of 0.134(3).

The rhodium(I) acetylidyde complex Rh(^{DiPP}PDI)(CCH) (**Rh_{CCH}**) could likewise be prepared by salt metathesis with ethynylmagnesium chloride. Single crystal X-ray crystallography confirms its structure, with a N_{py}–Rh bond length of 1.926(2) Å and a δ (PDI) value of 0.124(2).

As with **Co_{CO}⁺** and **Co_{CNBu}⁺**, cationic rhodium(I) carbonyl and isocyanide complexes could be prepared by halide abstraction. Reaction of 1,2-DFB solutions of **Rh_{Cl}** and Na[BAr^F₄] with CO or ³BuNC resulted in the formation of [Rh(^{DiPP}PDI)(CO)][BAr^F₄] (**Rh_{CO}⁺**) and [Rh(^{DiPP}PDI)(CN[−]Bu)][BAr^F₄] (**Rh_{CNBu}⁺**), respectively. Single crystal X-ray diffraction reveals a N_{py}–Rh bond length of 1.969(2) Å and a δ (PDI) of 0.161(3) for **Rh_{CO}⁺**, and a N_{py}–Rh bond length of 1.942(3) Å and a δ (PDI) of 0.152(3) for **Rh_{CNBu}⁺**.

To provide further points of comparison, the solid-state structures of the known rhodium(I) complexes Rh(^{DiPP}PDI)Cl (**Rh_{Cl}**), Rh(^{DiPP}PDI)Me (**Rh_{Me}**),³⁴ and [Rh(^{DiPP}PDI)(C₂H₄)][BAr^F₄] (**Rh_{ethene}⁺**),³⁷ were measured by single crystal X-ray diffraction. This allowed their N_{py}–Rh bond lengths and δ (PDI) values to be

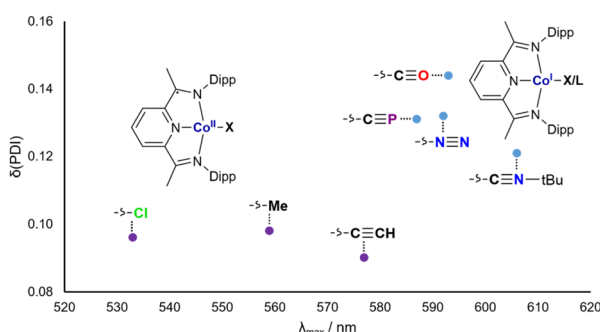


Fig. 5 UV-vis absorbance maxima (λ_{max}) plotted against δ (PDI) for **Co_X** and **Co_L⁺**.

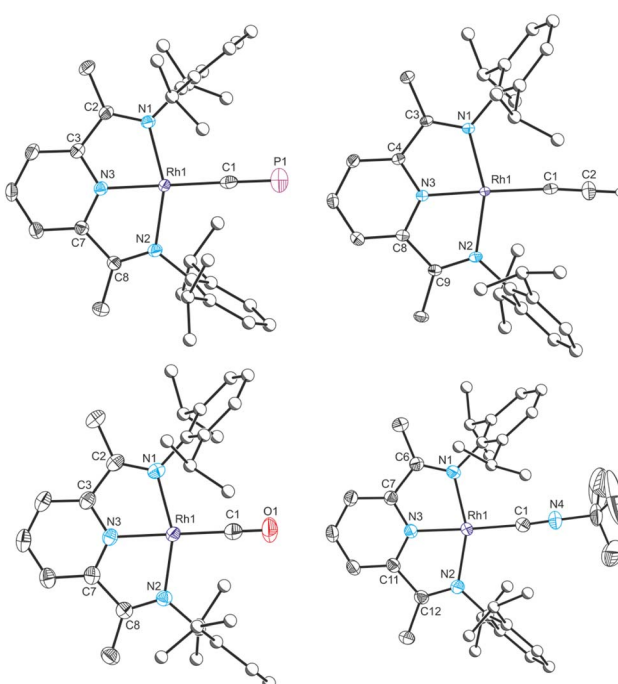


Fig. 6 Clockwise from top left: single crystal X-ray structures of complexes **Rh_{CP}**, **Rh_{CCH}**, **Rh_{CNBu}⁺** and **Rh_{CO}⁺**. Thermal ellipsoids set at 50% probability level. Hydrogen atoms (except for acetylidyde protons) removed for clarity. Atoms of Dipp groups pictured as spheres of arbitrary radius. Selected bond distances (Å) and angles (°) for **Rh_{CP}**: Rh1–C1 1.969(3), C1–P1 1.542(4), Rh1–N1 2.019(2), Rh1–N2 2.023(2), Rh1–N3 1.942(2), N1–C2 1.309(4), C2–C3 1.470(4), C3–N3 1.360(4), N3–C7 1.357(4), C7–C8 1.468(4), C8–N2 1.315(4); C1–Rh1–N1 101.06(11), C1–Rh1–N2 101.41(11), C1–Rh1–N3 179.24(14), N1–Rh1–N2 157.48(10), N1–Rh1–N3 78.92(10), N2–Rh1–N3, 78.59(10).



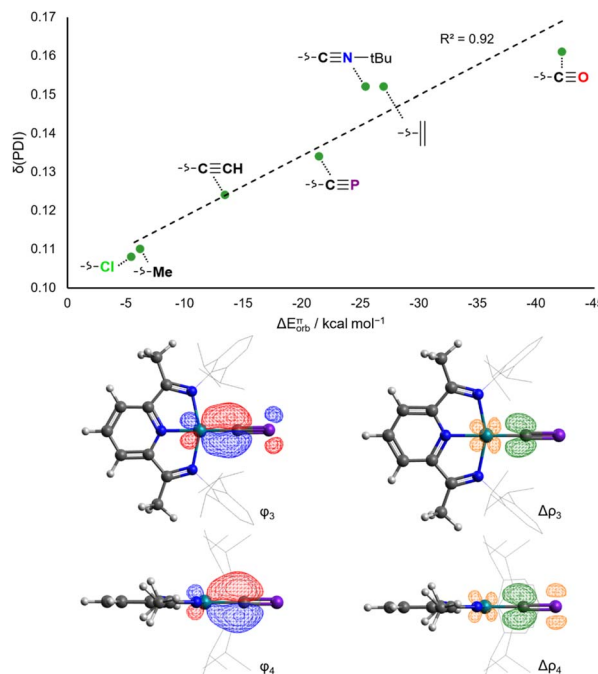


Fig. 7 Correlation of calculated ETS-NOCV π backdonation energies with experimental $\delta(\text{PDI})$ values for Rh_X and Rh_L^+ (top). Isosurfaces for the π bonding NOCVs and difference densities in Rh_{CP} (bottom).

determined: $\text{N}_{\text{py}}\text{-Rh} = 1.898(4)$ Å, and $\delta(\text{PDI}) = 0.108(6)$ for Rh_{Cl} , $\text{N}_{\text{py}}\text{-Rh} = 1.936(3)$ Å, and $\delta(\text{PDI}) = 0.110(6)$ for Rh_{Me} , $\text{N}_{\text{py}}\text{-Rh} = 1.960(2)$ Å, and $\delta(\text{PDI}) = 0.152(3)$ for $\text{Rh}_{\text{ethene}}^+$.

In contrast to the situation for the analogous cobalt complexes, the $\delta(\text{PDI})$ values for all the aforementioned Rh_X and Rh_L^+ complexes vary continuously with different ligands (Fig. 7). Changes to $\delta(\text{PDI})$ represent different degrees of rhodium(i) to $\text{Di}^{\text{pp}}\text{PDI}$ π backdonation, and consequently are highly sensitive to the π donor/acceptor properties of L. The π donor ligand Cl^- in Rh_{Cl} results in a low $\delta(\text{PDI})$ value (0.108(6)), whereas the strong π acceptor CO results in a high $\delta(\text{PDI})$ value (0.161(3)) in Rh_{CO}^+ . Calculated ETS-NOCV π backdonation energies ($\Delta E_{\text{orb}}^{\pi}$) correlate very well with $\delta(\text{PDI})$, as do calculated NBO π backdonation energies from 2nd order perturbation theory ($E^{(2)}\pi$). The $\text{N}_{\text{py}}\text{-Rh}$ bond length also varies with the *trans*-influence of L, though is also sensitive to σ donating ability, as evidenced by the anomalously high $\delta(\text{PDI})$ for Rh_{Me} (Fig. S58†).

The rhodium(i) cyaphide complex Rh_{CP} has a $\delta(\text{PDI})$ of 0.134(3) and $\text{N}_{\text{py}}\text{-Rh}$ bond length of 1.943(2) Å. This is likewise reflected in its calculated $\Delta E_{\text{orb}}^{\pi}$ (−21.5 kcal mol⁻¹) and $E^{(2)}\pi$ (44.1 kcal mol⁻¹) values. This places the π accepting ability of the cyaphide ion as being higher than the acetylide ion and almost as high as isocyanides, though still lower than neutral, strong π accepting ligands (e.g. CO, C₂H₄).

Conclusions

The cyaphide ion is both a strong σ donor and π acceptor in the terminal, κC coordination mode. The relatively low electronegativity of phosphorus makes the cyaphide ion a slightly stronger

σ donor than the cyanide and acetylide ions, and its low energy 2p-3p C≡P π^* orbitals make it a potent π acceptor despite its negative charge, with a π acidity comparable to neutral isocyanides. This will undoubtedly have consequences for using the cyaphide ion as a tool to tune the properties of coordination complexes. In particular, its strong π accepting ability in both the η^1 , κC coordination mode as well as the side-on η^2 coordination mode will make the cyaphide ion especially suitable for use as a bridging ligand in magnetic coordination polymers, for example heavy analogues of Prussian blue.

Data availability

Crystallographic data has been deposited with the Cambridge Structural Database.

Author contributions

Conceptualization: J. M. G.; experimental work: E. S. Y. and E. C.; X-ray crystallography: E. S. Y and J. M. G.; computational work: E. S. Y.; writing – original draft: E. S. Y and J. M. G.; writing & editing: all authors; supervision: E. S. Y. and J. M. G.; funding acquisition: J. M. G.

Conflicts of interest

There are no conflicts to declare.

Acknowledgements

We thank the University of Oxford, the EPSRC, and OxICFM CDT for financial support of this research (ESY: EP/S023828/1). The University of Oxford is also acknowledged for access to Chemical Crystallography and Advanced Research Computing (ARC) facilities.

Notes and references

† See ESI for full experimental details, analytical and computational data.

- 1 E. Gail, S. Gos, R. Kulzer, J. Lorösch, A. Rubo, M. Sauer, R. Kellens, J. Reddy, N. Steier and W. Hasenpusch, in *Ullmann's Encyclopedia of Industrial Chemistry*, Wiley-VCH, Weinheim, 2011, pp. 673–704.
- 2 O. Sato, T. Iyoda, A. Fujishima and K. Hashimoto, *Science*, 1996, **272**, 704–705.
- 3 A. Simonov, T. De Baerdemaeker, H. L. B. Boström, M. L. Ríos Gómez, H. J. Gray, D. Chernyshov, A. Bosak, H. B. Bürgi and A. L. Goodwin, *Nature*, 2020, **578**, 256–260.
- 4 L. M. Cao, D. Lu, D. C. Zhong and T. B. Lu, *Coord. Chem. Rev.*, 2020, **407**, 1–18.
- 5 E. S. Koumousi, I. R. Jeon, Q. Gao, P. Dechambenoit, D. N. Woodruff, P. Merzeau, L. Buisson, X. Jia, D. Li, F. Volatron, C. Mathonière and R. Clérac, *J. Am. Chem. Soc.*, 2014, **136**, 15461–15464.

6 J. A. Valdez-Moreira, A. E. Thorarinsdottir, J. A. Degayner, S. A. Lutz, C. H. Chen, Y. Losovsky, M. Pink, T. D. Harris and J. M. Smith, *J. Am. Chem. Soc.*, 2019, **141**, 17092–17097.

7 M. Lorenzi, J. Gellett, A. Zamader, M. Senger, Z. Duan, P. Rodríguez-Maciá and G. Berggren, *Chem. Sci.*, 2022, **13**, 11058–11064.

8 H. Jun, V. G. Young and R. J. Angelici, *J. Am. Chem. Soc.*, 1992, **114**, 10064–10065.

9 M. Finze, E. Bernhardt, H. Willner and C. W. Lehmann, *Angew. Chem., Int. Ed.*, 2004, **43**, 4160–4163.

10 J. G. Cordaro, D. Stein, H. Rüegger and H. Grützmacher, *Angew. Chem., Int. Ed.*, 2006, **45**, 6159–6162.

11 M. C. Levis, K. G. Pearce and I. R. Crossley, *Inorg. Chem.*, 2019, **58**, 14800–14807.

12 T. Görlich, D. S. Frost, N. Boback, N. T. Coles, B. Dittrich, P. Müller, W. D. Jones and C. Müller, *J. Am. Chem. Soc.*, 2021, **143**, 19365–19373.

13 D. L. Lichtenberger, S. K. Renshaw and R. M. Bullock, *J. Am. Chem. Soc.*, 1993, **115**, 3276–3285.

14 J. E. McGrady, T. Lovell, R. Stranger and M. G. Humphrey, *Organometallics*, 1997, **16**, 4004–4011.

15 S. K. Furfari, M. C. Leech, N. Trathen, M. C. Levis and I. R. Crossley, *Dalton Trans.*, 2019, **48**, 8131–8143.

16 D. W. N. Wilson, S. J. Urwin, E. S. Yang and J. M. Goicoechea, *J. Am. Chem. Soc.*, 2021, **143**, 10367–10373.

17 E. S. Yang and J. M. Goicoechea, *Angew. Chem., Int. Ed.*, 2022, **61**, e202206783.

18 M. L. H. Green and G. Parkin, *J. Chem. Educ.*, 2014, **91**, 807–816.

19 H. V. Huynh, Y. Han, R. Jothibasu and J. A. Yang, *Organometallics*, 2009, **28**, 5395–5404.

20 P. de Frémont, N. Marion and S. P. Nolan, *J. Organomet. Chem.*, 2009, **694**, 551–560.

21 S. Gaillard, A. M. Z. Slawin and S. P. Nolan, *Chem. Commun.*, 2010, **46**, 2742–2744.

22 C. M. Zinser, F. Nahra, L. Falivene, M. Brill, D. B. Cordes, A. M. Z. Slawin, L. Cavallo, C. S. J. Cazin and S. P. Nolan, *Chem. Commun.*, 2019, **55**, 6799–6802.

23 E. Y. Tsui, P. Müller and J. P. Sadighi, *Angew. Chem., Int. Ed.*, 2008, **47**, 8937–8940.

24 V. J. Scott, J. A. Labinger and J. E. Bercaw, *Organometallics*, 2010, **29**, 4090–4096.

25 M. R. Fructos, T. R. Belderrain, P. de Frémont, N. M. Scott, S. P. Nolan, M. Mar Díaz-Requejo and P. J. Pérez, *Angew. Chem., Int. Ed.*, 2005, **44**, 5284–5288.

26 C. Dash, P. Kroll, M. Yousufuddin and H. V. R. Dias, *Chem. Commun.*, 2011, **47**, 4478–4480.

27 L. Canovese, F. Visentin, C. Levi and V. Bertolasi, *Organometallics*, 2011, **30**, 875–883.

28 S. Gaillard, P. Nun, A. M. Z. Slawin and S. P. Nolan, *Organometallics*, 2010, **29**, 5402–5408.

29 C. Boehme and G. Frenking, *Organometallics*, 1998, **17**, 5801–5809.

30 D. Marchione, L. Belpassi, G. Bistoni, A. Macchioni, F. Tarantelli and D. Zuccaccia, *Organometallics*, 2014, **33**, 4200–4208.

31 C. Römel, T. Weyhermüller and K. Wieghardt, *Coord. Chem. Rev.*, 2019, **380**, 287–317.

32 M. J. Humphries, K. P. Tellmann, V. C. Gibson, A. J. P. White and D. J. Williams, *Organometallics*, 2005, **24**, 2039–2050.

33 V. C. Gibson, M. J. Humphries, K. P. Tellmann, D. F. Wass, A. J. P. White and D. J. Williams, *Chem. Commun.*, 2001, **1**, 2252–2253.

34 Q. Knijnenburg, D. Hetterscheid, T. Martijn Kooistra and P. H. M. Budzelaar, *Eur. J. Inorg. Chem.*, 2004, **2004**, 1204–1211.

35 Q. Knijnenburg, A. D. Horton, H. Van Der Heijden, T. M. Kooistra, D. G. H. Hetterscheid, J. M. M. Smits, B. De Bruin, P. H. M. Budzelaar and A. W. Gal, *J. Mol. Catal. A: Chem.*, 2005, **232**, 151–159.

36 S. Nückel and P. Burger, *Organometallics*, 2001, **20**, 4345–4359.

37 E. L. Dias, M. Brookhart and P. S. White, *Organometallics*, 2000, **19**, 4995–5004.

